

Thermodynamics using Wilson and Staggered Quarks

E. Laermann^a

^aFakultät für Physik, Universität Bielefeld, Postfach 100 131, 33501 Bielefeld, Germany

Recent developments in QCD at finite temperature are reviewed. Particular emphasis is laid on results stemming from simulations which involve quarks.

1. INTRODUCTION

Lattice investigations of QCD at finite temperature have contributed considerably to the current understanding of the transition from the hadronic state of matter to the quark gluon plasma and of the physics of the plasma phase. Mainly due to the ever-present limitations of computational power many analyses have been carried out in the pure gauge sector of QCD such that bulk properties of gluons at finite temperature can be regarded as solved: the system has a well-established first-order transition [1], the equation of state is known in the continuum limit [2] and the critical temperature in the continuum limit has been determined with only a few percent uncertainty [3,4]. Clearly, more detailed questions like e.g. the nature of excitations in the plasma deserve further work, also in the quenched approximation. Yet, the emphasis of recent research has shifted towards studies of full QCD including staggered as well as Wilson quarks. These studies consistently have lead to an estimate of the critical temperature of order 150 MeV for 2 flavors so far. This value is considerably lower than the quenched number of $T_c = 270(5)\text{MeV}$. Through the relation $T = 1/(aN_\tau)$ of the temperature T to lattice spacing a and temporal extent N_τ of the lattice, dynamical fermion simulations in the vicinity of the transition are, at a given N_τ , carried out at considerably larger lattice spacings. Already for that reason, with the standard discretizations, extrapolations to the continuum limit will be more difficult than in the quenched case. Therefore, the search for improved actions has received much attention recently in the context of finite temperature QCD.

This review attempts to summarize the developments in finite temperature lattice QCD since last year's conference as reviewed in [5]. I will concentrate on problems and results in simulations with full QCD. Section 2 summarizes estimates of the critical temperature. In section 3 the present status of knowledge about the nature of the chiral transition is discussed, mainly for two flavors staggered as well as Wilson fermions. Section 4 describes studies of energy density and pressure in the high temperature limit while section 5 reviews a few recent results on screening lengths and masses. This year's results at finite density are summarized in section 6, conclusions are given in section 7.

2. CRITICAL TEMPERATURE

One of the basic quantities to be derived from finite temperature lattice QCD is the value of the critical temperature. In order to prepare the stage for the subsequent discussion of results from dynamical fermion simulations, Figure 1 summarizes the current status of analysis in the quenched approximation [4]. Figure 1 shows the ratio $T_c/\sqrt{\sigma}$ where σ is the string tension extracted from the static quark potential for various actions. For all data points the value of the critical coupling has been extrapolated to its infinite (spatial) volume limit at which then the string tension was determined. The lowest set of data points originates from simulations with the standard Wilson gauge action [2,4]. A quadratic extrapolation in the lattice spacing to the continuum limit gives $T_c/\sqrt{\sigma} = 0.631(2)$. Symanzik-improved actions show a much weaker cut-off dependence and are in agreement with the

continuum extrapolation of the standard action [4,6] Likewise, the results [3] from Iwasaki's RG-improved action are consistent with a constant behavior in a , but they deliver a value of the critical temperature of $T_c/\sqrt{\sigma} = 0.656(4)$ which is about 3% higher than the number from the standard action. Since the procedure to extract the string tension has not been the same for the two numbers, one might suspect that the difference in the quoted value for T_c , $T_c = 276(2)\text{MeV}$ versus $266(2)\text{ MeV}$, is mainly due to differences in the analysis of the static quark potential [7] rather than to differences in the improvement scheme.

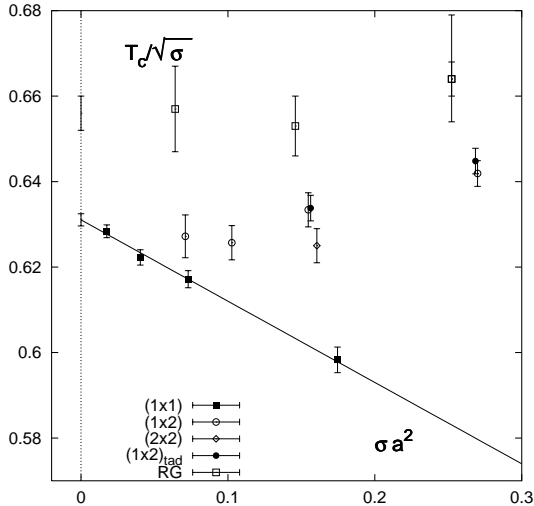


Figure 1. The quenched critical temperature in units of the square root of the string tension for various gauge actions versus the the lattice spacing squared.

The current situation with dynamical fermions is depicted in Figure 2. The plot summarizes data from simulations with 2 flavors of quarks, staggered fermions at $N_\tau = 4$ and 6 [8,9] as well as improved Wilson fermions at $N_\tau = 4$ [8], plus $N_F = 4$ staggered results obtained from $N_\tau = 4$ lattices with an improved action [10] in addition to an old number [11] from $N_\tau = 8$ and a standard action. Compared to the equivalent quenched plot, Figure 2 shows that the lattice spacings at

which T_c has been determined so far are considerably larger than in pure gauge theory simulations. Moreover, the investigations have not been carried out at the physical quark masses. The arrow in Figure 2 indicates that at fixed N_τ the transition takes place at larger lattice spacings when the quark mass is decreased. Thus the critical temperature is decreasing when the quark mass is lowered.

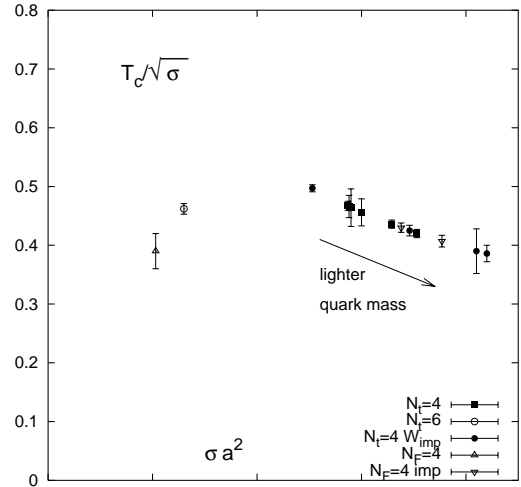


Figure 2. The critical temperature in units of the square root of the string tension for dynamical fermions versus the square of the lattice spacing (for further explanations see text).

The same data is shown again as a function of the pseudoscalar Goldstone boson to vector meson mass ratio $(M_{PS}/M_V)^2$ in Figure 3. (The meson masses at the appropriate critical values of the coupling in parts have been obtained by means of a phenomenological interpolation formula [12].) Here now, at fixed N_τ , smaller lattice spacings are to the right of the figure. The $N_\tau = 4$ staggered data indicates that T_c over $\sqrt{\sigma}$ tends to lower values as the quark mass is decreased. The same trend is observed for the Wilson improved results, although at larger $(M_{PS}/M_V)^2$ ratio. On the other hand, the $N_\tau = 6$ data point seems to indicate that, at a given quark mass, de-

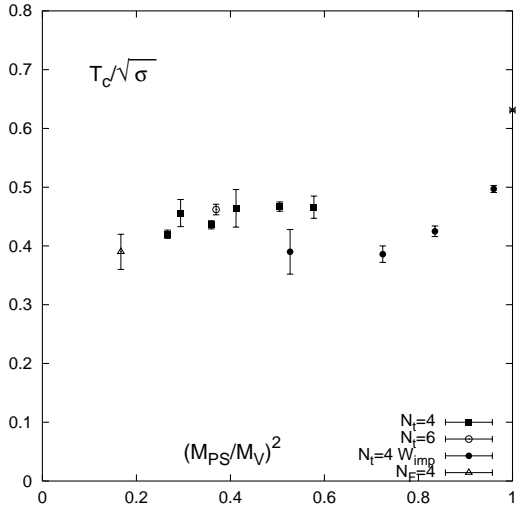


Figure 3. The critical temperature in units of the square root of the string tension for dynamical fermions plotted versus $(M_{PS}/M_V)^2$. The point at $(M_{PS}/M_V)^2 = 1$ is the $N_\tau = 4$ quenched value.

creasing the lattice spacing increases $T_c/\sqrt{\sigma}$ only slightly. At the moment, one would therefore estimate a physical value for the critical temperature of $T_c/\sqrt{\sigma} \lesssim 0.4$ or $T_c \lesssim 170\text{MeV}$.

The critical temperature has also been estimated from the ratio to the vector meson mass. In this case one ought to go (close) to the chiral limit in order to extract a physical number. In the case of using the string tension to set the scale one might argue that the string tension is considerably less affected by the quark mass. Figure 4 shows T_c/M_V for $N_F = 2$ staggered fermions [9,13–16,12], plotted as function of $(M_{PS}/M_V)^2$. As the quark mass is decreased this ratio rises. Recall that the infinite quark mass, quenched data point corresponds to $M_{PS}/M_V = 1$ and $T_c/M_V = 0$. As the lattice spacing is decreased, T_c/M_V stays remarkably constant. Extrapolating the $N_\tau = 4$ data to the chiral limit suggests a value of $T_c/M_V \simeq 0.2$ or $T_c \simeq 150\text{MeV}$. Note that this value disagrees somewhat with the number extracted from the string tension.

The corresponding data for dynamical Wilson quarks [8,17–19] are given in Figure 5. Despite the known problems with standard Wilson

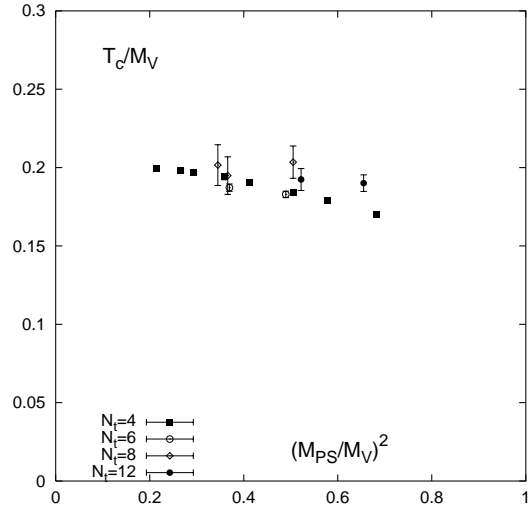


Figure 4. The critical temperature in units of the vector meson mass for staggered fermions plotted versus $(M_{PS}/M_V)^2$.

fermion thermodynamics, at least the results for $N_\tau = 6$ and 8 as well as the first data with improved Wilson fermions [8] are not in disagreement with the staggered data.

3. PHASE TRANSITION

3.1. Staggered $N_F = 2$: critical behavior

The theoretical expectations on the scaling behavior of the theory at the chiral transition are based on the σ model in three dimensions. For the case of two light flavors, if the transition is second order, it is expected to show scaling behavior with $SU(2) \times SU(2) \simeq O(4)$ exponents. On the other hand, if the anomalous $U_A(1)$ symmetry were effectively restored, the relevant symmetry group would be $U_A(1) \times SU(2) \times SU(2) \simeq O(2) \times O(4)$ and the transition could be first order [20].

It has been attempted to analyze the critical behavior of 2 flavor staggered QCD by studying the scaling behavior of various quantities and determining critical exponents [21]. These scaling relations are derived from the scaling of the singular part of the free energy density,

$$f(t, h) = -\frac{T}{V} \ln Z = b^{-1} f(b^{y_t} t, b^{y_h} h) \quad (1)$$

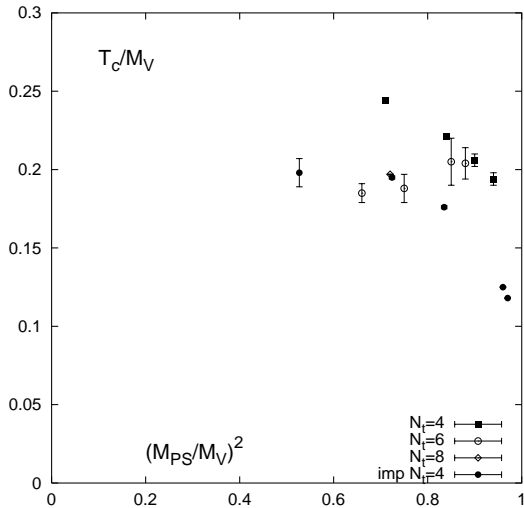


Figure 5. The critical temperature in units of the vector meson mass for Wilson fermions versus $(M_{PS}/M_V)^2$.

Here T and V denote temperature and volume, Z is the partition function, t is the reduced temperature, $t = (T - T_c)/T_c$, and h is the symmetry breaking field, $h = m/T$ where m is the quark mass. The scaling factor b is arbitrary and can be chosen appropriately. In the vicinity of the critical point thermodynamic quantities should be governed by the thermal (y_t) and the magnetic (y_h) critical exponent. In the staggered version of lattice regularized QCD, for the dimensionless couplings t and h one uses

$$\begin{aligned} t &= \frac{6}{g^2} - \frac{6}{g_c^2(0)} \\ h &= maN_\tau \end{aligned} \quad (2)$$

where $g_c(0)$ denotes the critical coupling on a lattice with fixed temporal extent in the limit of vanishing quark mass. At non-vanishing quark mass, a pseudo-critical coupling $g_c(m)$ is defined as the location of a peak in e.g. the Polyakov loop susceptibility.

The status of investigations of the chiral transition with two light staggered quarks has been commented upon at last year's conference [5]. Since then, JLQCD [22] as well as the Bielefeld group [23] have about finalized their analyses. A

new analysis was presented by C. DeTar at this conference [24].

The quantities analyzed by JLQCD and the Bielefeld group are various susceptibilities, in particular the magnetic or chiral susceptibility

$$\chi_m = \frac{T}{V} \sum_{i=1}^{N_F} \frac{\partial^2}{\partial m_i^2} \ln Z \quad (3)$$

and the thermal susceptibility

$$\chi_t = -\frac{T}{V} \sum_{i=1}^{N_F} \frac{\partial^2}{\partial m_i \partial (1/T)} \ln Z \quad (4)$$

Assuming that the free energy is dominated by its singular part, Eq. (1) then leads to the scaling predictions for the peak heights of the susceptibilities at the line of pseudo-critical couplings

$$\begin{aligned} \chi_m^{\text{peak}} &\sim m^{-z_m} \\ \chi_t^{\text{peak}} &\sim m^{-z_t} \end{aligned} \quad (5)$$

where the exponents are given by $z_m = 2 - 1/y_h$ and $z_t = (y_t - 1)/y_h + 1$. The pseudo-critical line itself is expected to follow

$$\frac{6}{g_c^2(m)} = \frac{6}{g_c^2(0)} + cm^{z_g} \quad (6)$$

with $z_g = y_t/y_h$. The values of these exponents for various symmetries [25] are given in table 1. At finite lattice spacing the exact chiral symmetry of the staggered fermion action is $U(1) \simeq O(2)$. However, sufficiently close to the continuum limit one expects $O(4)$ exponents. The possibility of mean-field (MF) exponents arbitrarily close to the transition has been raised by [26].

Earlier investigations of the exponents on small lattices ($8^3 \times 4$) had observed partial agreement with $O(4)$ scaling [21]. These studies have been repeated on larger spatial volumes, $L = 12, 16$. In addition to the quark mass values 0.02, 0.0375 and 0.075 JLQCD also ran at $m = 0.01$. The volume dependence of the chiral peak susceptibility is shown in Figure 6, similar results are available for the other quantities. For $m \geq 0.02$, the susceptibility rises when the volume is increased from 8^3 to 12^3 , but then stays approximately constant. Thus, a phase transition does not occur in this mass range, in agreement with earlier claims [27].

Table 1

Critical exponents for $O(2)$, $O(4)$ and mean field (MF). The 2 flavor QCD results are given separately for each spatial lattice size, with upper values denoting the JLQCD and the lower ones the Bielefeld group numbers.

	O(2)	O(4)	MF	L=8	L=12	L=16
z_g	0.60	0.54	2/3	0.70(11)	0.74(6)	0.64(5)
z_m	0.79	0.79	2/3	0.70(4)	0.99(8)	1.03(9)
				0.84(5)	1.06(7)	0.93(8)
z_t	0.39	0.34	1/3	0.47(5)	0.81(9)	0.83(12)
				0.63(7)	0.94(12)	0.85(12)

At $m = 0.01$ the linear increase in the peak height as the volume is enlarged continues up to $L = 16$. As such, this observation could suggest a first order transition. JLQCD however have studied the volume dependence of a double-peak structure in the distribution of the chiral order parameter and conclude that a first order transition is likely to be absent [22].

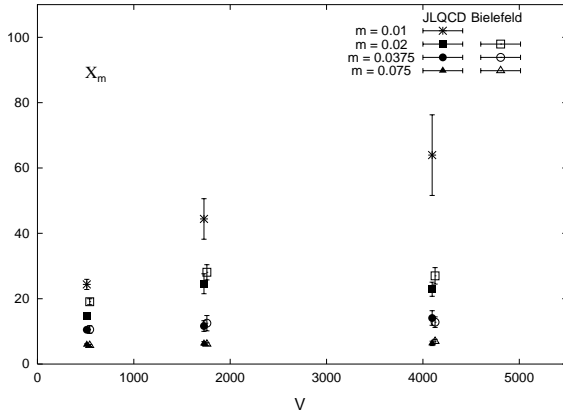


Figure 6. Volume dependence of the chiral susceptibility at peak.

The quark mass dependence of χ_m^{peak} is shown in Figure 7, together with fits to the expected scaling behavior, Eq. (5). The resulting values for the critical exponents are also summarized in

Table 1. For z_g , within two standard deviations agreement with all three predictions is obtained. For the other two exponents, both groups consistently observe a drastic change when the volume is increased from $L = 8$ to $L = 12, 16$. While for the small volume the value for z_m is in rough agreement with $O(2)$ and $O(4)$, the results from $L = 12$ and 16 do not agree with any of the predicted numbers. Indeed, the observed value $z_m \simeq 1$ would be expected for a first order transition. The thermal exponent z_t is larger than any of the predictions for all volumes.

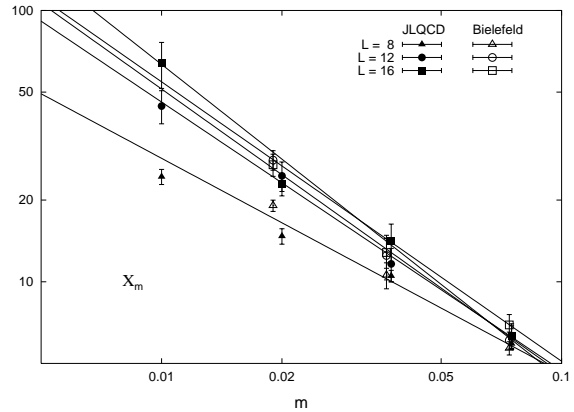


Figure 7. Mass dependence of the chiral susceptibility at peak. The upper 4 lines are fit results with Eq. (5) to the $L = 12$ and 16 data while the lowest line shows the slope of $O(4)$ scaling.

Another way to study the scaling behavior is to compute the (magnetic) equation of state [28]

$$\langle \bar{\psi}\psi \rangle h^{-1/\delta} = \phi(th^{-1/\beta\delta}) \quad (7)$$

and compare it with the scaling function ϕ as determined from a parametrization of $O(4)$ simulation results [29], after adjusting two non-universal normalization constants. This has been done by the MILC Collaboration [24] for $N_\tau = 4, 6, 8$ and 12. The result for $N_\tau = 4$ is shown in Figure 8. While the data for the larger quark masses and smaller volumes are compatible with $O(4)$, the new data at smaller quark masses and larger lattice extent again show drastic disagreement.

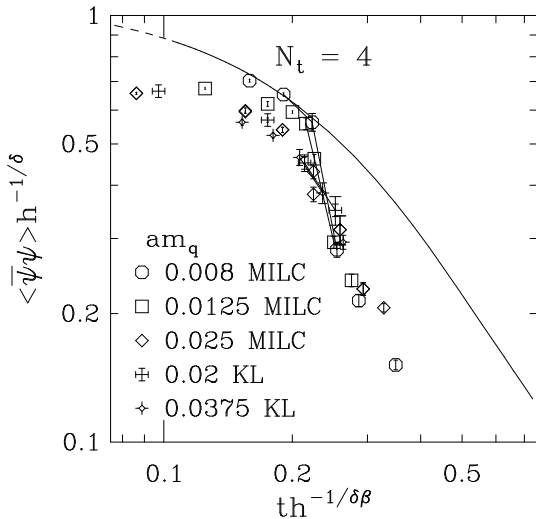


Figure 8. The magnetic equation of state, Eq. (7), at $N_\tau = 4$ [24]. The data at quark masses 0.0375, 0.02 and 0.025 comes from $L = 8$ lattices while at 0.0125 and 0.008 lattice extents up to $L = 24$ have been used. The line is the $O(4)$ scaling prediction. It can be moved horizontally as well as vertically by adjusting two free normalization constants.

(MILC also has looked at one of the exponents, with the result $z_t = 1.3(2)$.) When N_τ is increased, thus going to smaller lattice spacings, the agreement becomes increasingly better [24], but it should be remarked that the data at $N_\tau = 12$ originates from quark mass values $m/T \simeq 0.1$ which are of about the same size as the larger quark masses used at $N_\tau = 4$. Also, even at large spacing one would expect $O(2)$ behavior which is indistinguishable from $O(4)$ with the current precision of the data.

At the moment there is no convincing explanation for these discrepancies at hand. In view of the results presented in section 3.3 obtained with an improved gauge action and Wilson fermions one might speculate that at strong coupling and for the standard action the relation Eq. (2) between the QCD parameters and the thermodynamic variables as they enter the singular part of the free energy is strongly distorted. More studies at weaker coupling or with improved actions

would be needed to solve this important question.

3.2. $U_A(1)$ restoration

The nature of the chiral transition for two flavors is strongly affected by the realization of the $U_A(1)$ symmetry [20]. At very high temperatures topologically non-trivial configurations are suppressed, thus leading to the effective restoration of the symmetry despite the anomaly. For 2 light quark flavors the effective restoration of $U_A(1)$ is reflected in the degeneracy of the pion and the isovector-scalar $a_0(\delta)$ mass [30]. This degeneracy can also be detected by comparing the correlation functions

$$\omega = \int d^4x (\langle \pi(x)\pi(0) \rangle - \langle a_0(x)a_0(0) \rangle) \quad (8)$$

If $U_A(1)$ is restored this quantity should vanish in the chiral limit. The (generalized) susceptibility has been looked at by various groups [31,32,23]. At finite quark mass ω is dropping across the chiral transition, but stays non-zero above T_c . Figure 9 shows the latest Columbia data for this quantity, together with various extrapolations to the chiral limit.

In the continuum, the susceptibility ω is expected to be an analytic and, for $N_F = 2$, even function in the quark mass. Indeed, fits with a quadratic m dependence work and lead to a finite intercept in the chiral limit. However, the data look strikingly linear and fitting them with a linear ansatz results in a vanishing of the susceptibility at $m = 0$. At finite lattice spacing, due to zero-mode shifts and taking the square root of the determinant the approach towards the chiral limit is not so clear [32]. Therefore one should continue to study the quark mass dependence at even smaller quark masses as well as at smaller lattice spacings.

The approach chosen in [33,34] is to determine screening masses. Above the critical temperature, the difference between π and a_0 mass drops considerably, but a non-degeneracy remains at finite quark mass, thus confirming the findings originating from the analysis of the susceptibility. In order to address the problem of the chiral limit from a different angle, ref. [34] also computed the lowest eigenvalues λ and corresponding eigenvectors ψ_λ of the fermion matrix. In the continuum,

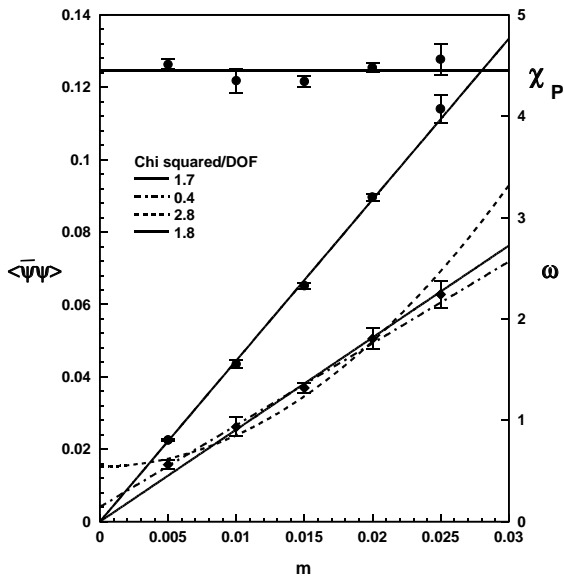


Figure 9. The quantity ω , Eq. (8), which measures the breaking of the $U_A(1)$ symmetry plotted versus the quark mass (lowest data) together with various fits [32]. Also shown are the results for the integrated pion correlator, χ_P , and the chiral condensate. The data were obtained on a $16^3 \times 4$ lattice at fixed β slightly above β_c .

in the phase symmetric with respect to the axial $SU(2)$, the chiral limit of ω is given by the zero-modes,

$$\omega = \left\langle \sum_{\lambda=0} \frac{\bar{\psi}_\lambda \gamma_5 \psi_\lambda}{i\lambda + m} \right\rangle \quad (9)$$

In [34] it is then verified that ω obtained in the standard fashion is saturated by the contribution from low eigenmodes thus supporting that continuum arguments seem to hold at lattices spacings of $\mathcal{O}(0.15\text{fm})$ ($N_\tau = 8$). The contribution of zero modes in Eq. (9) is to leading order quark mass independent. If this could be verified e.g. by running at more quark mass values the results of [34] would indicate that the $U_A(1)$ symmetry is not restored at the chiral transition.

3.3. Wilson fermions $N_F = 2$

The phase diagram of QCD at finite temperature with 2 flavors of Wilson quarks has been clarified in [35] and has been explained in great detail in last year's review [5]. At finite N_τ , the line $\kappa_c(\beta)$ defined through the vanishing of the pion mass starts off at $1/4$ at $\beta = 0$ and extends to $\kappa_c \simeq 0.22$ at about $\beta \simeq 4.0$ where it bends backwards again to the region of stronger couplings (see also [36]). On the other hand, coming from the confined phase, at the thermal line $\kappa_t(\beta)$ where the Polyakov loop develops a non-vanishing expectation value the pion mass increases rapidly due to the approximate restoration of chiral symmetry. Only in the region where the thermal line is close to κ_c does the theory have a pion with a small mass. Thus, the chiral transition can only be explored in that region. Unfortunately, this region is at strong coupling for $N_\tau = 4$ and moves towards smaller coupling only very slowly with increasing temporal extent of the lattice [37], rendering a study of the transition in the vicinity of continuum physics prohibitively expensive. For that reason and for the well-known pathologies [19] several groups have started to work with improved actions.

Iwasaki et al. simulated with the standard Wilson fermion action but on RG-improved glue [38]. Qualitatively, the phase diagram is very similar to the standard one so that small pion masses again are obtained in the vicinity of the finite temperature κ_c cusp. In addition to the phase diagram the group has also investigated the magnetic equation of state, Eq. (7). For Wilson fermions quark mass and chiral order parameter have to be obtained from chiral Ward identities [39]. This involves renormalization constants for which the lowest order perturbative values have been used in [38]. The results, including new data at low β are shown in Figure 10. The agreement with the $O(4)$ scaling curve is remarkable. The analysis was carried out on lattices of size $8^3 \times 4$ and with mainly not very small quark masses. It would be very interesting to continue the investigation on larger lattices and with more data at smaller quark masses.

The MILC Collaboration has analyzed the finite temperature transition with the Symanzik-

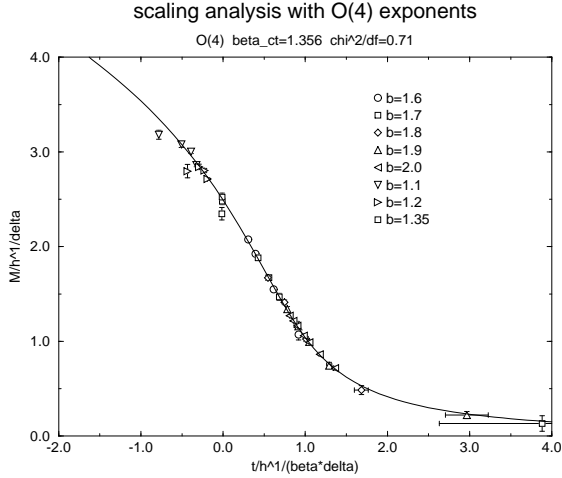


Figure 10. The magnetic equation of state, Eq. (7), with two flavors of standard Wilson fermions on improved glue [38].

Lüscher-Weisz gluon action in combination with the Sheikholeslami-Wohlert fermion action, both tadpole improved [8]. They obtain a much smoother cross-over behavior as compared with the standard actions which suggests that the pathologies of the latter are lattice artefacts. The results for meson masses and the string tension have been presented already in section 2. Also Bielefeld started to work with Wilson fermions. Preliminary results on the phase diagram for tree level-improved glue and the clover action were presented at this conference [40]. Qualitatively, the behavior of the κ_c and κ_t lines is very similar to the standard one.

3.4. Wilson fermions $N_F \neq 2$

The phase diagram has also been studied for the number of flavors differing from 2. All analyses have been carried out with standard Wilson fermions on lattices with $N_\tau = 4$ so far.

The case $N_F = 1$ has been looked at in [41]. For heavy quarks the deconfinement transition shows first order behavior as a finite size analysis of the Polyakov loop reveals. The first-order transition weakens when the quark mass is decreased. The end-point of the transition is estimated to occur at about 1.1 GeV.

The cases $N_F = 3$ and 4 have been studied in Tsukuba [42]. In both cases the phase diagram is very similar to the one with 2 flavors, in particular the κ_c line forms a cusp. Regarding the nature of the chiral transition, for $N_F \geq 3$ one expects first order in the continuum limit [20]. At large quark masses, away from the cusp, one indeed observes first order behavior. When the quark mass is lowered however, the $N_F = 4$ data shows a weakening of first-order signals. For $N_F = 3$, one has to use an approximate algorithm e.g. the Hybrid R. At a time step size of $\delta\tau = 0.01$ two-state signals were observed also close to κ_c . These signals weaken when the time discretization errors of the algorithm are decreased ($\delta\tau = 0.005$). Thus, for both $N_F = 3$ and 4 the order of the transition is still unclear.

4. EQUATION OF STATE

Thermodynamic quantities like pressure or energy density receive substantial contributions from high momentum modes, $p = \pi T$. Since on the lattice these are distorted by UV cut-off effects e.g. the energy density in the infinite temperature limit deviates considerably from the continuum Stefan-Boltzmann value. For the pure gauge theory in the standard Wilson discretization the corrections are

$$\epsilon_0^G = \epsilon_{SB}^G \left[1 + \frac{10}{21} \left(\frac{\pi}{N_\tau} \right)^2 + \frac{2}{5} \left(\frac{\pi}{N_\tau} \right)^4 + \mathcal{O} \left(\left(\frac{\pi}{N_\tau} \right)^6 \right) \right] \quad (10)$$

This effect is even larger for the fermionic part of the energy with standard staggered quarks,

$$\epsilon_0^F = \epsilon_{SB}^F \left[1 + \frac{465}{441} \left(\frac{\pi}{N_\tau} \right)^2 + \mathcal{O} \left(\left(\frac{\pi}{N_\tau} \right)^4 \right) \right] \quad (11)$$

On the other hand, the signal for this quantity vanishes proportional to $1/N_\tau^4$. Bulk thermodynamic quantities were investigated in the standard discretization, both quenched [2] and with 2 flavors of staggered quarks [43]. While for the quenched theory it was possible to extrapolate to the continuum, in view of the analytic results,

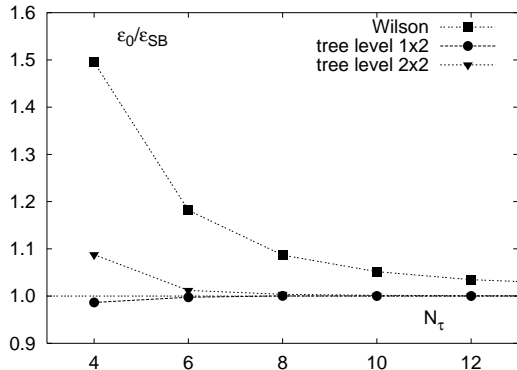


Figure 11. The gluonic part of the energy density at high temperature computed on lattices with finite temporal extent in units of the continuum Stefan-Boltzmann value for various gauge actions [44].

Figures 11,12, this seems to be very difficult with dynamical fermions.

In the infinite temperature, Stefan-Boltzmann limit, cut-off effects are reduced at tree level. Perturbative or tadpole improvements do not have any effect in this limit. The size of the remaining corrections to the Stefan-Boltzmann limit can be read off Figures 11,12 where a variety of different actions are compared with each other [44,45].

The effect of various improvement schemes at temperatures as low as the critical temperature has been tested in quenched simulations [46]. For the pressure, it seems that tree level improvement is the leading effect, although one would have expected that close to the transition infrared modes and their improvement would be more important. Tadpole improvement seems to have an effect though for the interface tension [47].

A first attempt to analyze bulk thermodynamic quantities by means of an improved fermion discretization scheme, the Naik action, has been published recently [10]. At the moment, there are investigations underway which try to estimate the effect of various improvement strategies on the restoration of flavor symmetry [48–50,45]. It remains to be seen how much this would help to extract energy density or pressure closer to the continuum limit at finite temperatures.

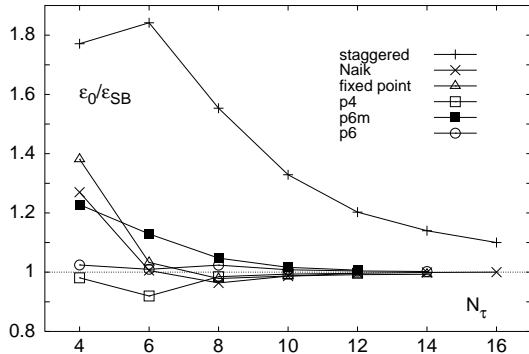


Figure 12. The fermionic part of the energy density at high temperature computed on lattices with finite temporal extent in units of the continuum Stefan-Boltzmann value for various staggered fermion actions [45].

5. SCREENING LENGTHS AND MASSES

The study of hadronic excitations at finite temperature is an important subject as it reveals more details about the properties of the plasma phase as well as the approach to the transition where temperature dependencies could mimic plasma signatures.

The temperature dependence of pseudoscalar and vector meson (screening) masses has been studied in [51]. The masses were determined at temperatures slightly below and above the transition, $T \simeq 0.9T_c$ and $T \simeq 1.2T_c$ respectively, and compared with zero temperature results. The investigation was carried out with the Sheikholeslami-Wohlert fermion action applied to quenched gauge configurations. The results, obtained in the quark mass region ranging from light to approximately the charm quark masses do not exhibit any strong temperature effect for $0.9T_c$. At $1.2T_c$ the data are approaching the high temperature, free quark limit, $M_{\pi,\rho} \lesssim 2\pi T$. This confirms earlier results for staggered fermions [52].

Heavy quarks at temperatures around the critical one are investigated in [53]. The heavy quarks in the range $m_c < m < m_b$ are simulated by means of an NRQCD action applied to quenched

configurations which have been generated with a (1×2) tree level improved gauge action. The propagation of quarkonia states is followed in the time direction. For that purpose, the investigation is carried out on anisotropic lattices with a large anisotropy ratio $\xi = a_\sigma/a_\tau = 4.65$ in order to have enough Matsubara frequencies. So far, the analysis was done for the 3S_1 ground and first excited state. Below T_c , at about $0.8T_c$ no temperature effect was seen. At $1.2T_c$, the propagator which is dominated by the ground state at large time separations t from the source becomes flatter than the zero temperature propagator at large t . This effect can be interpreted as a decrease in the mass by a small amount of about 12 MeV at the lightest quark mass simulated. The effect becomes weaker with increasing quark mass. The first excited state, projected on by the same trial wave function as at $T = 0$, undergoes a larger change of about - 240 MeV at the charm quark mass. At least qualitatively, the results are in accord with the expectations from a Debye-screened potential model, namely that smaller states feel the screening less.

Investigations of the Debye mass itself have been presented by [54,55]. The aim of both groups is to confront the lattice data with perturbative results. It is known since long [56] that high temperature QCD is plagued by infrared divergencies. These are cured at $\mathcal{O}(gT)$ by the Debye or electric gluon mass m_e . It is widely believed that the magnetic mass m_m is non-vanishing and acquires a value of $\mathcal{O}(g^2T)$. Such a mass would solve the infrared problem at this order but cannot be calculated in perturbation theory. If m_m is non-vanishing next-to-leading order perturbation theory predicts [57] for the electric mass

$$m_e^2 = m_{e0}^2 \left(1 + g \frac{N}{2\pi} \sqrt{\frac{6}{2N + N_F}} \left[\ln \frac{2m_e}{m_m} - \frac{1}{2} \right] \right) \quad (12)$$

where m_{e0} denotes the leading term $m_{e0} = \sqrt{N/3 + N_F/6}gT$. The methods used by [54] and [55] are quite different. In [54] dimensional reduction is applied and the 3d effective theory is simulated. The Debye mass is then extracted from the correlation of a gauge-invariant operator [58].

The authors of [55] generate $SU(2)$ gauge configurations with the standard as well as an improved action. They analyze gauge-variant gluon and Polyakov loop correlations after fixing to Landau gauge. Their data show a non-vanishing magnetic gluon mass which varies with temperature according to $m_m(T) = cg^2(T)T$. For the electric mass, the results of the two groups differ somewhat quantitatively. However, both groups show clearly that (next-to-leading order) perturbation theory describes the data only at very large temperatures of $\mathcal{O}(10^4T_c)$.

6. QCD AT FINITE DENSITY

It is well known that at finite chemical potential $\mu \neq 0$ the effective action of QCD becomes complex. This prohibits the use of standard Monte Carlo methods to evaluate the path integral. A way to circumvent these difficulties is provided by what is known as the Glasgow method [59]. This method was applied to QCD at intermediate and recently at strong coupling [60]. In the latter case mean-field computations [61] and results from a monomer-dimer simulation [62] are available. The results of [60] show a finite density transition at a critical value μ_c which agrees with the mean-field as well as with the monomer-dimer number. However, also an onset μ_o at which the number density starts to deviate strongly from 0 is observed. The value of μ_o coincides with $m_\pi/2$ for smaller quark masses so that in the chiral limit the chiral condensate would immediately drop from its zero chemical potential value when μ is increased from 0. Similar findings were obtained at intermediate coupling. The same behavior was also seen in the quenched approximation where it was traced back to the failure of this approximation at finite μ [63]. The reason for this behavior in full QCD is not clear. One might speculate [59] that sampling configurations at $\mu = 0$ might not catch the right physics at finite μ . Similar observations on μ_o were reported in [64] where the modulus of the determinant was used in the partition function. A different approach has been presented in [65] where perturbatively irrelevant four-fermion interactions were added to the QCD action. This way one is able to

simulate at vanishing bare quark mass, but it has to be clarified yet whether this approach really produces only physical results.

7. CONCLUSIONS

The results of last year's research on finite temperature lattice QCD with dynamical quarks have been reviewed. At currently accessible quark masses the critical temperature for 2 flavors is being estimated as around 150 MeV. This number is, not unexpectedly, quite smaller than the quenched value of 270(5) MeV. Correspondingly, at fixed N_τ the computations with quarks have been carried out at considerably larger lattice spacings compared to quenched simulations. Moreover, going to lighter quarks drives one to stronger coupling. One may speculate that lattice spacing effects are the reason for the very unexpected behavior at the chiral/deconfinement transition for both standard staggered and Wilson fermions while improving only the gauge part already seems to lead to remarkable agreement with the theoretical predictions. In addition, the computation of the energy density of a free fermion gas shows that the discretization effects can be large for fermions when the standard lattice transcriptions are used. Thus it is highly desirable to find improved actions for the analysis of the thermodynamics with quarks.

ACKNOWLEDGEMENTS

It is a pleasure to thank my colleagues at Bielefeld, B. Beinlich, A. Bicker, J. Engels, F. Karsch, C. Legeland, M. P. Lombardo, M. Lütgemeier, M. Oevers, A. Peikert, B. Petersson, J. Rank, K. Rummukainen and P. Schmidt as well as S. Aoki, I. Barbour, K. Bitar, G. Boyd, N. Christ, C. DeTar, J. Fingberg, Y. Iwasaki, S. Kaya, J.-F. Lagaë, S. Morrison, M. Okawa and A. Ukawa for (preliminary) data, plots, discussions and sharing their insight.

REFERENCES

1. A.Ukawa, Nucl.Phys. B(Proc.Suppl.)17 (1990) 118 and references therein.
2. G.Boyd et al., Phys.Rev.Lett. 75 (1995) 4169, Nucl.Phys. B469 (1996) 419.
3. Y.Iwasaki et al., hep-lat/9610023v3
4. B.Beinlich et al., hep-lat/9707023.
5. A. Ukawa, Nucl. Phys. B (Proc. Suppl.) 53 (1997) 106.
6. G.Cella et al., Phys.Lett. B333 (1994) 457.
7. C.Legeland, these proceedings.
8. MILC Collaboration, hep-lat/9703003.
9. Bielefeld results, unpublished.
10. J.Engels et al., Phys.Lett. B396 (1997) 210.
11. K.D.Born et al., Phys.Lett. B329 (1994) 325.
12. C.Bernard et al., Phys.Rev. D54 (1996) 4585.
13. S.Gottlieb et al., Phys.Rev.Lett. 59 (1987) 1513.
14. C.Bernard et al., Phys.Rev. D45 (1992) 3854.
15. HTMC GC Collaboration, Phys.Rev. D47 (1993) 3619; Nucl.Phys. B(Proc.Suppl.)30 (1993) 315.
16. R.Mawhinney, Nucl.Phys. B(Proc.Suppl.)30 (1993) 331.
17. K.M.Bitars et al., Phys.Rev. D43 (1991) 2396.
18. C.Bernard et al., Phys.Rev. D46 (1992) 4741.
19. T.Blum et al., Phys.Rev. D50 (1994) 3377.
20. R.D.Pisarski and F.Wilczek, Phys.Rev. D29 (1984) 338; F.Wilczek, Int.J.Mod.Phys. A7 (1992) 3911; K.Rajagopal and F.Wilczek, Nucl.Phys. B399 (1993) 395.
21. F.Karsch, Phys.Rev. D49 (1993) 3791; F.Karsch and E.Laermann, Phys.Rev. D50 (1994) 6954.
22. A.Ukawa, these proceedings; JLQCD Collaboration, Tsukuba workshop, hep-lat/9708010.
23. E.Laermann, Tsukuba workshop.
24. C.DeTar, these proceedings; see also D.Toussaint, Tsukuba workshop.
25. G.A.Baker, B.G. Nickel and D.I.Meiron, Phys.Rev. B17 (1978) 1365; J.C.Le Guillou and J.Zinn-Justin, Phys.Rev. B21 (1980) 3976; K.Kanaya and S.Kaya, Phys.Rev. D51 (1995) 2404.
26. A.Kocić and J.B.Kogut, Phys.Rev.Lett. 75 (1995) 3109; Nucl.Phys. B455 (1995) 229.
27. M.Fukugita et al., Phys.Rev.Lett. 65 (1990) 816; Phys.Rev. D42 (1990) 2936; F.R.Brown et al., Phys.Rev.Lett. 65 (1990) 2491.
28. C. DeTar, Nucl. Phys. B (Proc. Suppl.) 42

- (1995) 73.
29. D. Toussaint, Phys.Rev. D55 (1997) 362.
 30. E.V.Shuryak, Comments Nucl.Phys. 21 (1994) 235; S.H.Lee and T.Hatsuda, Phys.Rev. D54 (1996) 1871; N.Evans, S.D.H.Hsu and M.Schwetz, Phys.Lett. B375 (1996) 262; M.C.Birse, T.D.Cohen and J.A.McGovern, Phys.Lett. B388 (1996) 137.
 31. C.Bernard et al., Phys.Rev.Lett. 78 (1997) 598.
 32. N.Christ, Tsukuba workshop.
 33. S.Gottlieb et al., Phys.Rev. D55 (1997) 6852.
 34. J.-F.Lagaë, these proceedings; J.B.Kogut, J.-F.Lagaë and D.K.Sinclair, Nucl.Phys. B(Proc.Suppl.)53 (1997) 269.
 35. S.Aoki, A.Ukawa and T.Umemura, Phys. Rev.Lett. 76 (1996) 873 and references therein.
 36. K.Bitár, these proceedings; Phys.Rev. D56 (1997) 2736.
 37. Y.Iwasaki et al., Phys.Rev. D54 (1996) 7010.
 38. S.Kaya, these proceedings, Y.Iwasaki et al., Phys.Rev.Lett. 78 (1997) 17.
 39. M.Bochicchio et al., Nucl.Phys. B262 (1985) 331; S.Itoh et al., Nucl.Phys. B274 (1986) 33.
 40. M.Oevers, these proceedings.
 41. C.Alexandrou, these proceedings; C.Alexandrou et al., Nucl.Phys. B(Proc. Suppl.) 53 (1997) 435.
 42. S.Aoki, Tsukuba workshop, hep-lat/9707020 and references therein; S.Aoki et al., private communication.
 43. MILC Collaboration, Phys.Rev. D55 (1997) 6861.
 44. F.Karsch, Tsukuba workshop, hep-lat/9706006.
 45. A.Peikert, these proceedings.
 46. B.Beinlich, these proceedings.
 47. B.Beinlich, F.Karsch and A.Peikert, Phys. Lett. B390 (1997) 268.
 48. Y.Luo, these proceedings; hep-lat/9702013.
 49. D.Sinclair, these proceedings.
 50. T.Blum et al., Phys.Rev. D55 (1997) 1133.
 51. P.Schmidt, these proceedings.
 52. F.Karsch, Nucl.Phys. B(Proc.Suppl.)34 (1994) 63 and references therein.
 53. J.Fingberg, these proceedings; hep-lat/9707012.
 54. K.Rummukainen, these proceedings; K.Kajantie et al., hep-ph/9708207.
 55. J.Rank, these proceedings, U.Heller, F.Karsch and J.Rank, hep-lat/9708009.
 56. A.D.Linde, Phys.Lett. B96 (1980) 289.
 57. A.K.Rebhan, Phys.Rev. D48 (1993) R3967.
 58. P.Arnold and L.G.Yaffe, Phys.Rev. D52 (1995) 7208.
 59. for a recent review see I.M.Barbour et al., Tsukuba workshop, hep-lat/9705042.
 60. M.-P.Lombardo, these proceedings; M.-P.Lombardo, hep-lat/9611004; I.M.Barbour et al, hep-lat/9705038.
 61. N.Bilic, K.Demeterfi and B.Petersson, Nucl. Phys. B377 (1992) 615.
 62. F.Karsch and K.Mütter, Nucl.Phys. B313 (1989) 541.
 63. A.Gocksch, Phys.Rev. D37 (1988) 1014; M.A.Stephanov, Phys.Rev.Lett. 76 (1996) 4472.
 64. A.Galante, these proceedings.
 65. S.E.Morrison, these proceedings; I.M.Barbour, S.E.Morrison and J.B.Kogut, hep-lat/9612012.